Nano Res (2008) 1: 403–411
DOI 10.1007/s12274-008-8040-5
Research Article

Preparation of Monodisperse Se Colloid Spheres and Se Nanowires Using Na_2SeSO_3 as Precursor

Liping Liu, Qing Peng, and Yadong Li (✉)

Department of Chemistry, Tsinghua University, Beijing 100084, China

Received: 3 September 2008 / Revised: 19 September 2008 / Accepted: 19 September 2008

ABSTRACT

Nearly monodisperse spherical amorphous Se colloids are prepared by the dismutation of Na_2SeSO_3 solution at room temperature; by altering the pH of the solution, amorphous Se colloid spheres with sizes of about 120 nm, 200 nm, 300 nm, and 1 μm can be obtained. Se@Ag_2Se core/shell spheres are successfully synthesized by using the obtained amorphous Se (a-Se) spheres as templates, indicating the potential applications of these Se nanomaterials in serving as soft templates for other selenides. Meanwhile, selenium nanowires are obtained through a "solid-solution-solid" growth process by dispersing the prepared Se spheres in ethanol. This simple and environmentally benign approach may offer more opportunities in the synthesis and applications of nanocrystal materials.

KEYWORDS

Na_2SeSO_3, dismutation, amorphous Se (a-Se) spheres, trigonal Se (t-Se) nanowires

Introduction

Materials which are composed of the element selenium play important roles in the fields of photonics and electronics due to its special photoconductive properties [1, 2]; the electrical conductivity of selenium can be enhanced by several orders of magnitude when it is exposed to visible light, and it has been applied in photodetectors or sensors, photocopy machines, and electrical rectifiers [1, 3]. Selenium also has many attractive physical and chemical properties that may be beneficial in the field of optical applications, such as a relatively high refractive index and a high solubility in various solvents like CS_2 or N_2H_4 [3], which makes it a potential candidate for fabricating three-dimensional photonic crystals or inverse opaline structures, as it is easily removed [4, 5]. Furthermore, selenium is a relatively active material and can react with a variety of chemical reagents to form other materials, such as Ag_2Se, and CdSe [1, 6, 7], which possess wide potential applications as soft templates for functional selenides.

In the past few years, a number of methods have been reported for the preparation of Se nanomaterials including spherical colloids and one-dimensional structures. Most of these have focused on trigonal-phase selenium (t-Se) one-dimensional structures [8–13], as they can be conveniently synthesized in large quantities with uniform size due to the inherent anisotropic crystal structure of Se. In contrast, the preparation of Se colloidal spheres has been less

Address correspondence to ydli@mail.tsinghua.edu.cn

discussed. The formation of spherical Se is generally only possible if the element retains an amorphous structure, which is thermodynamically unstable, and meticulous synthetic methods are required to obtain such a-Se spheres. The phase transformation energy from amorphous selenium to trigonal selenium is only 6.63 kJ / mol, and the glass transition temperature is around 31 °C [1], and thus slightly forcing reaction conditions or temperature will lead to a phase transformation from the a-Se to t-Se. The main methodology which has been adopted for the preparation of a-Se spheres is aqueous chemical reduction. Selenous acid and sodium selenite are the most frequently used precursors in these reduction methods, and several different reducing agents have been used, such as hydrazine, glutathione, ascorbic acid, and sodium thiosulfate [14–18], as shown in the following equation:

$$H_2SeO_3 + N_2H_4/Na_2S_2O_3/C_6H_8O_6 \xrightarrow{\text{equeous}} Se$$

The reduction of selenium precursors to form Se spheres has also been achieved by γ-irradiation [19]. However, few of these methods are able to prepare Se colloid spheres with satisfactory sizes and size distribution. In addition, selenous acid and sodium selenite are very toxic precursors, and careful operations are needed in the experiment and the final treatment. Very recently, Xia and co-workers [20] have reported the synthesis of uniform a-Se spheres by reducing selenous acid with hydrazine in ethylene glycol. Moreover, by changing the molar ratio of selenous acid and hydrazine, a-Se spheres with diameters from ~90 nm to 420 nm can be obtained.

In this work, we introduce another simple synthetic route and an environmentally benign precursor, Na_2SeSO_3, as Se source to prepare uniform a-Se spheres. Na_2SeSO_3 is sensitive to the acidity of the solution. It can be synthesized by refluxing Se powder and Na_2SO_3 in an alkaline aqueous solution, while the dismutation phenomenon (which can separate out elemental selenium) will occur when it is in a neutral or acidic solution at room temperature. The transformation of the Na_2SeSO_3 is shown as follows:

$$Na_2SeSO_3 \underset{pH>8.5}{\overset{pH<8.0}{\rightleftharpoons}} Na_2SO_3 + Se$$

Thus, by controlling the reaction conditions, Se powder can be transformed into Na_2SeSO_3 by reacting with Na_2SO_3 in alkaline aqueous solution, and then separated out as a-Se spheres by dismutation of the Na_2SeSO_3 in acidic solution; the pH of the solution, which will influence the dismutation rate of the Na_2SeSO_3, can be utilized to adjust the diameter of the a-Se products.

1. Experimental

Materials. All reagents used in this work, including Se powder, Na_2SO_3, NaOH, oleic acid, and ethanol, were A. R. grade (>99.99%) from the Beijing Chemical Factory, China. The selenium source, Na_2SeSO_3 solution (0.1 mol/L), was prepared by refluxing 5 mmol selenium powder and 7 mmol Na_2SO_3 in 50 mL deionized water for 2 h.

Synthesis of a-Se spheres. In a typical synthesis, 0.2 g NaOH and 8.0 mL oleic acid were dissolved in a mixture of 10 mL deionized water and 15 mL C_2H_5OH to form a transparent solution, then 5 mL Na_2SeSO_3 solution (as prepared above) was added to this solution with stirring. The solution immediately changed from colorless to red, indicating the formation of the a-Se. The red color slowly changed to orange-red during the reaction. After about 45 min, the orange-red product was separated from the solution by centrifugation, and dried at room temperature to afford the final powdered product. The preparation of a-Se spheres with sizes of ~200 nm, ~300 nm, and ~1000 nm was carried out by changing the amount of the NaOH to 0.4 g, 0.6 g, and 0.9 g, respectively, with the other parameters in the reaction system remaining unchanged. Subsequent treatments of these products were similar to the above.

Synthesis of t-Se nanowires. After the dismutation of the Na_2SeSO_3 in the above reaction system, the precipitate of a-Se spheres was redispersed in ethanol solvent by stirring or sonication, and the solutions were kept at 50 °C for about 2 days. The resulting black products were separated by centrifugation or filtration, and dried at 50 °C to afford the final nanowire products.

Characterization. X-ray diffraction patterns were

recorded on a Bruker D8 Advance X-ray diffractometer (XRD) with Cu Kα radiation (λ =1.5418 Å). The sizes and the morphology of the as-prepared Se spheres and Se nanowires were examined by using a transmission electron microscope (JEOL JEM-1200EX), a scanning electron microscope (JSM-6301F) and high resolution transmission electron microscope (HRTEM, FEI Tecnai G2 F20 S-Twin, working at 200 kV). Raman spectra were recorded with an RM 2000 microscopic confocal Raman spectrometer (Renishaw PLC, UK) employing a 514 nm laser beam.

2. Results and discussion

Figure 1(a) shows the TEM image of the a-Se product obtained in the typical synthesis process, when 0.2 g NaOH and 8.0 mL oleic acid were used; the pH value of the solution was 6.08, and the Na_2SeSO_3 decomposed immediately at this acidity. Since the reaction temperature (~20 °C) was controlled below the glass transition temperature of selenium, all the elemental Se separated out was in amorphous form. It can be seen from Fig. 1(a) that the product is composed of nearly monodisperse nanocrystals with a diameter of about 120 nm, which usually self-assemble into two-dimensional arrays on the TEM grids. Since the amorphous form is not the stable phase of selenium, the product on the TEM grid tends to show a little melting under the strong electron beam. The melted a-Se product slowly fills in the interspaces between the nanoparticles, which makes the spherical particles look hexagonal in shape [21]. There are no detectable X-ray diffraction (XRD) peaks for the amorphous phase Se products [20]. Figure 1(b) shows the energy dispersive spectroscopy (EDS) result for the Se product. In the EDS, Se is the only element detected, indicating that the product is highly pure. Figure 1(c) shows the SEM micrograph of the a-Se product; the image reveals that the a-Se particles are all spherical with a mean diameter of 120 nm, which matches well with the TEM result in Fig. 1(a).

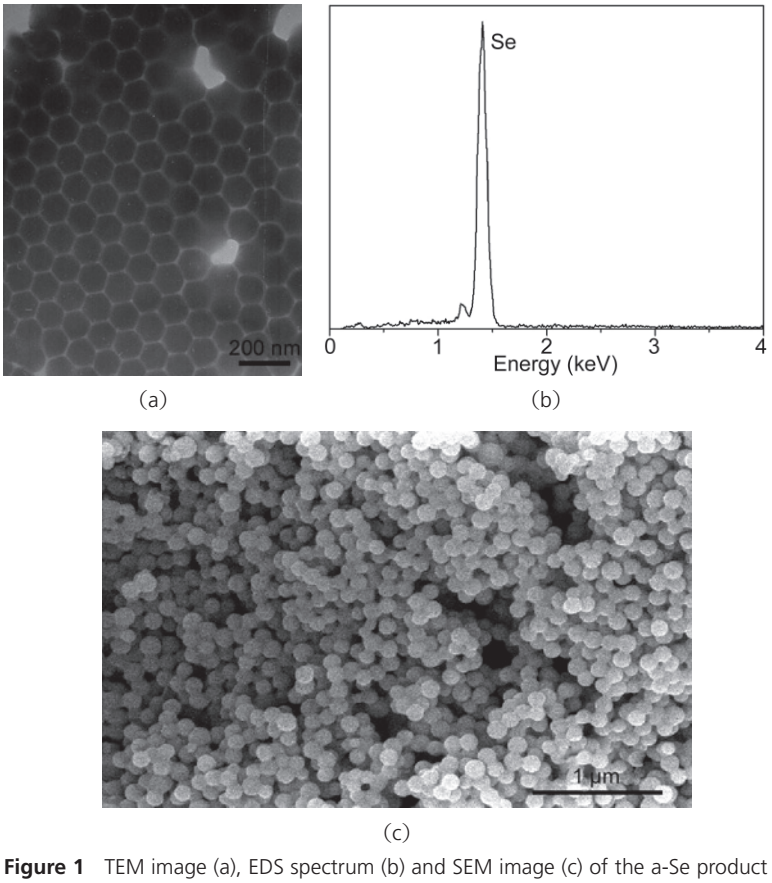

Figure 1 TEM image (a), EDS spectrum (b) and SEM image (c) of the a-Se product obtained in a typical synthesis with 0.2 g NaOH and 8.0 mL oleic acid (pH = 6.08)

Raman spectra of the a-Se products were also recorded. Selenium exists mainly in three polymorphs, the principal one being a trigonal phase, consisting of helical chains, with a less stable monoclinic phase, consisting of Se_8 rings, and amorphous selenium consisting of a mixture of disordered chains. These three different structures have Raman resonance peaks at ~235 cm^{-1}, ~256 cm^{-1}, and ~264 cm^{-1}, respectively [22]. Figure 2 displays the Raman spectrum of the a-Se powder product. Figure 2(a) is the result after the sample was scanned by the Raman laser for the first time, and Figure 2(b) is the result after the sample had been scanned several times. It can be seen that in Fig. 2(a) that the main peak is at ~236 cm^{-1}, with two lesser peaks at ~254 cm^{-1} and ~262 cm^{-1}. In Fig. 2(b), the peaks at 254 cm^{-1} and 262 cm^{-1} have almost disappeared, leaving the enhanced peak at 237 cm^{-1}. The change in Fig. 2 can be explained as follows: since the phase transformation energy from amorphous selenium to trigonal selenium is low, when the sample is

exposed to the Raman laser (a powerful energy beam), the amorphous form readily changes to the more stable ordered structure. Therefore, even when the Raman measurement was recorded for the first time, the amorphous Se had begun to change to the monoclinic phase and the trigonal phase, which resulted in the appearance of the three characteristic peaks in Fig. 2(a). When the laser had scanned the sample several times, the sample had completely transferred to the trigonal phase, explaining why only the characteristic peak of trigonal selenium at 237 cm^{-1} remained in Fig. 2(b). After the Raman measurements, the color of the sample that had been exposed to the laser changed from red to black when viewed in a microscope, consistent with the phase transformation of the a-Se.

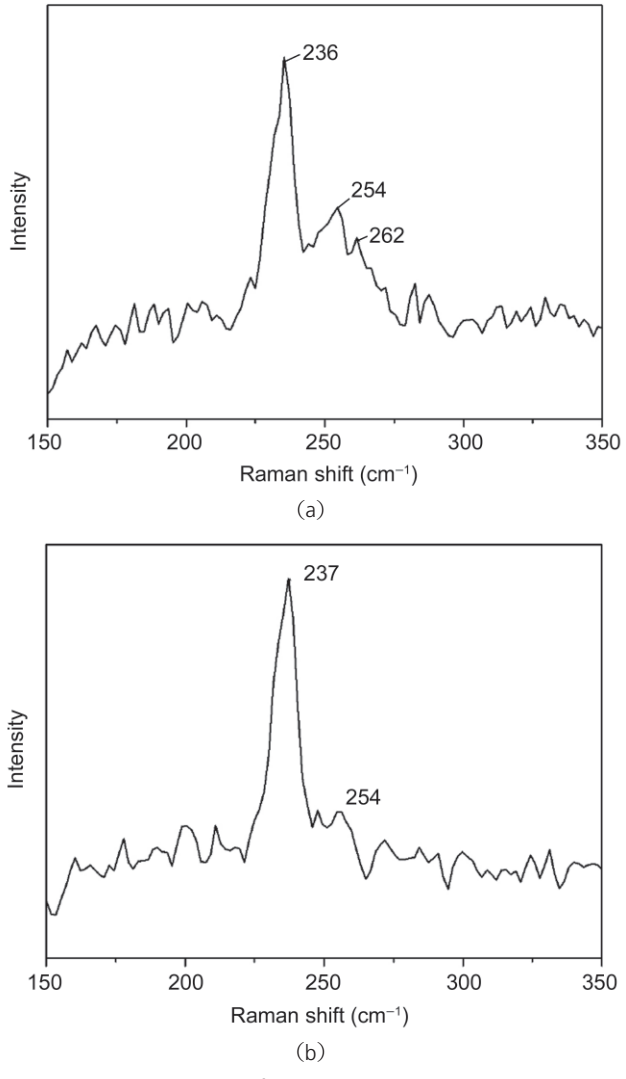

Figure 2 Raman spectra of the a-Se spheres scanned by the laser for the first time (a) and several times (b)

Since the stability of Na_2SeSO_3 is sensitive to the acidity, and the pH of the solution can influence the dismutation rate of the Na_2SeSO_3, it can be used to adjust the nucleation events of the a-Se formed by decomposition of the Na_2SeSO_3 and thus control the final diameter of the products. By varying the amount of the NaOH from 0.2 g to 0.4 g, 0.6 g, and 0.9 g with the other reaction parameters remaining the same, the pH value of the reaction solution changed from 6.08 to 6.44, 6.92, and 7.75, respectively, which led to the final diameter of the a-Se sphere products increasing from 120 nm to 200 nm, 300 nm, and 1 μm, as shown in Figs. 3(a), 3(c), and 3(d), respectively. The diameter changes of the a-Se spheres were evidently caused by the different dismutation rates of the Na_2SeSO_3 in environments with different acidity. In this dismutation reaction, it can be envisaged that more acidic solutions would lead to the faster dismutation rate of the Na_2SeSO_3 due to its inherent instability in acidic environments. The faster dismutation rate afforded larger amounts of the a-Se nuclei, resulting in the smaller size of the final products. In contrast, more alkaline solutions would lead to fewer a-Se nuclei and thus result in larger products. The different dismutation rates of the Na_2SeSO_3 can also be easily observed in the experiments. When Na_2SeSO_3 was added to the solution with pH value of 6.08, the colorless solution changed to red immediately; meanwhile in the solution with pH value of 7.75, the solution changed slowly from colorless to orange, then to the red, and this transformation process lasted for about 5 min. The dismutation rate of the Na_2SeSO_3 slowed down with increasing pH value, and if we further increased the pH value of the solution by adding an amount of NaOH beyond 1.0 g (pH>8.5) to the reaction, the dismutation phenomenon did not occur, showing that the Na_2SeSO_3 was stable in this relatively alkaline solution.

Besides the pH value of the solution, oleic acid also plays important role in controlling the size distribution of the products. When the amount of the NaOH and oleic acid was reduced to half of the quantity in the typical synthesis reaction, that is, using 0.1 g NaOH and 4.0 mL oleic acid dissolved in the mixture of deionized water and C_2H_5OH, the size

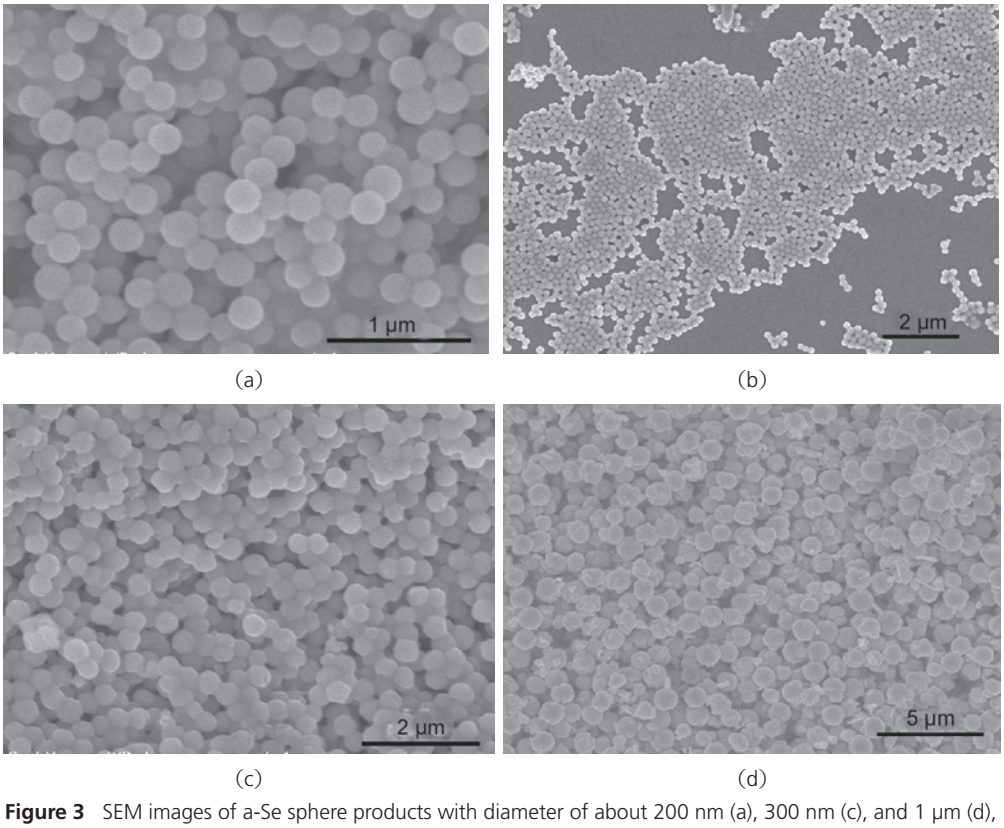

Figure 3 SEM images of a-Se sphere products with diameter of about 200 nm (a), 300 nm (c), and 1 μm (d), which were obtained in solutions with pH value of 6.44, 6.92, and 7.75, respectively. (b) SEM image when the a-Se spheres (200 nm) solution was dropped on the Si substrate

of the resulting products had a wide distribution, as shown in Fig. 4, although the pH value remained the same at 6.08 under these conditions. The effect of the oleic acid here could be to increase the viscosity of the solution, which is similar to the function of the more viscous solvent ethylene glycol in a previous report in the Ref. [20]. The oleic acid could ensure a better control over the processes—such as nucleation and growth kinetics—involved in the formation of elemental selenium, leading to the more uniform sized products. On the other hand, the sodium oleate (the product of reaction of oleic acid with sodium hydroxide) could also act as a surfactant, which could prevent the fine particles from aggregating irregularly.

As an effective synthesis strategy, the template-directed synthesis method is a powerful approach for generating products with specific shape. Since selenium can react with a variety of chemical reagents and be transformed into many other functional materials [1, 6, 7, 23–25], herein we chose Ag_2Se as an example to illuminate the template-directed synthesis of the a-Se products. Figure 5 shows the

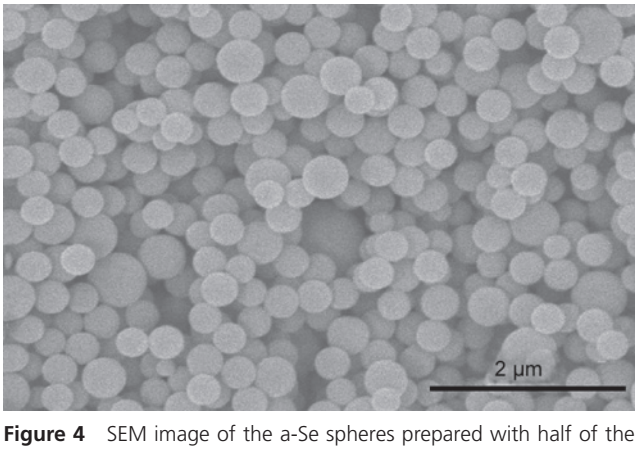

Figure 4 SEM image of the a-Se spheres prepared with half of the amount of the oleic acid used in the typical synthesis (see Fig. 1)

SEM micrograph and XRD pattern of the Se@Ag_2Se core/shell spheres obtained by reacting a-Se spheres with $AgNO_3$ in ethylene glycol as solvent in the presence of polyvinylpyrrolidone (PVP) (the average molecular weight, M_w=30 000). The reflections in the XRD pattern match well to orthorhombic β-Ag_2Se (JCPDS 24-1041), and there is still no reflection peak for elemental Se as the Se core is in the amorphous form. From Fig. 5(a) we can see that the Se@Ag_2Se

products retained almost the same uniform size as the a-Se spheres, which implies that these a-Se spheres can serve as effective soft templates for functional selenides.

Compared to the monodisperse a-Se spheres, the preparation of high quality t-Se nanowires is easier because the trigonal form is the stable phase of selenium and it has an anisotropic crystal structure which can guide the one-dimensional growth. Trigonal Se nanowires can be synthesized by the reduction of selenous acid [26–31] or the recrystallization of Se powder [32, 33]. In these two synthetic routes, the formation of t-Se nanowires mostly involves a transformation from a-Se (which is produced in the reaction) to the t-Se through a dissolution and sequential crystallization process, which is called the solid-solution-solid mechanism [26]. Herein, we directly used the a-Se spheres obtained above as a material to prepare t-Se nanowires through such a solid-solution-solid process. The preparation of the t-Se involved dispersion of the a-Se spheres in ethanol by stirring, followed by aging at 50 °C for about 2 days, which allows the a-Se to transform completely into the t-Se, and finally collection of the products by filtration.

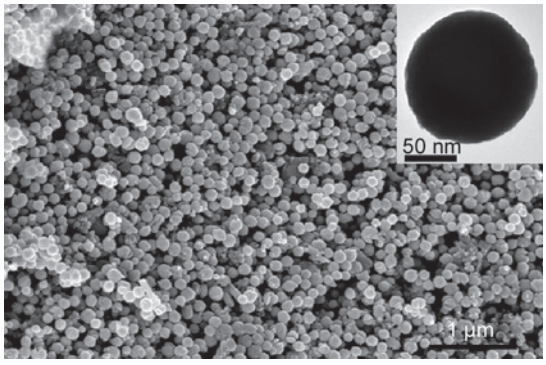

(a)

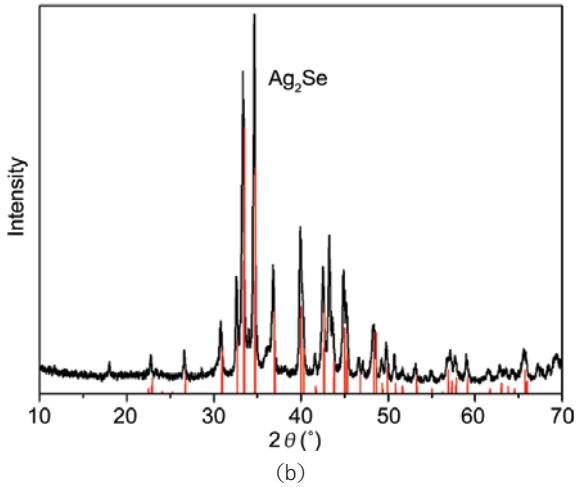

(b)

Figure 5 (a) SEM micrograph of the Se@Ag_2Se sphere products which were prepared by reacting the a-Se spheres with $AgNO_3$ in ethylene glycol solvent in the presence of PVP (M_w=30000). Inset is the TEM image of a single Se@Ag_2Se sphere. (b) XRD pattern of the Se@Ag_2Se. The reflections in the XRD pattern match well to orthorhombic β-Ag_2Se (JCPDS 24-1041). There is no peak for elemental Se as the Se core is in the amorphous form

XRD was used to characterize the composition and structure of the product. All the reflections in the XRD pattern in Fig. 6(a) match well to the trigonal phase of Se (JCPDS 73-0465). The Raman spectrum gives further evidence confirming the presence of the trigonal phase. Figure 6(b) shows a typical Raman spectrum of the as-prepared Se nanowires. Only one resonance peak at around 237 cm^{-1} is observed, without the appearance of the peaks at 256 cm^{-1} and 264 cm^{-1} during the Raman measurements, indicating a pure trigonal phase was present. Figure 6(c) shows an SEM image of the t-Se products. It can be seen that the t-Se products are nanowires with a mean diameter of 300 nm ± 30 nm and length of up to several micrometers, and no Se spheres are observed. In this conversion process, when the a-Se spheres were dispersed in ethanol, the a-Se gradually dissolved to form a metastable solution, and then the selenium atoms recrystallized on the t-Se seeds which were produced in the hot ethanol solvent because of the low solubility of the t-Se in ethanol [9]. At this time, the anisotropic characteristic of the t-Se provided a natural template to guide the growth of Se atoms along one particular axis, and thus the products turned out to be nanowires [27, 33, 34]. The solvent in which the a-Se is dispersed plays an important role in the Se nanowire growth in this conversion. If water was used instead of ethanol, only massive Se products were found instead of t-Se nanowires, and thus an appropriate solvent in which the solubility of a-Se is larger than that of t-Se is important to ensure conversion of the initial a-Se to the t-Se nanowires.

When the a-Se spheres were dispersed in ethanol by sonication, the t-Se nanowires obtained were thinner than those obtained after dispersion by stirring. From Fig. 7(a), it can be seen that the products are about 160 nm ± 20 nm in diameter and can grow up to several tens of micrometers.

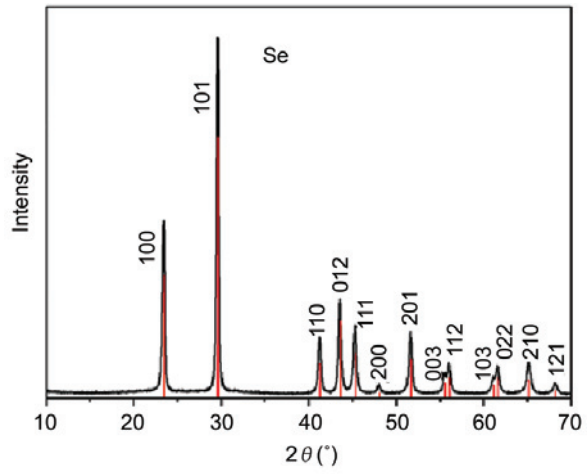

(a)

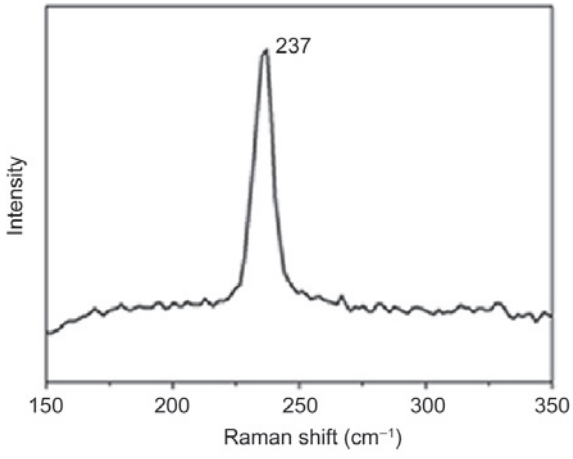

(b)

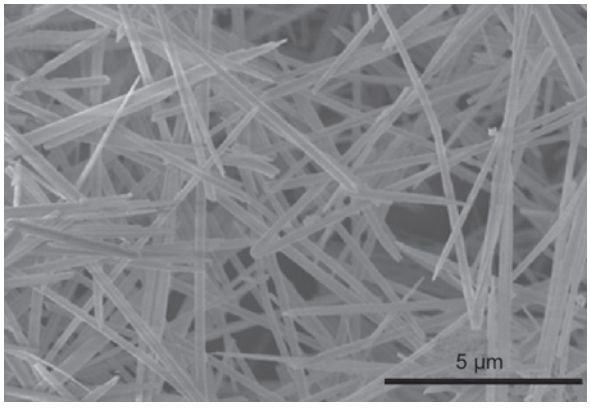

(c)

Figure 6 (a) XRD pattern of the Se nanowires; (b) Raman spectrum of the Se nanowires; (c) SEM image of the as-prepared t-Se nanowires

The spindly products produced here through the sonication process might be caused by the larger amounts of t-Se seeds present because the sonication process is known to induce the formation of such t-Se seeds [27]. Growth of the Se material on the

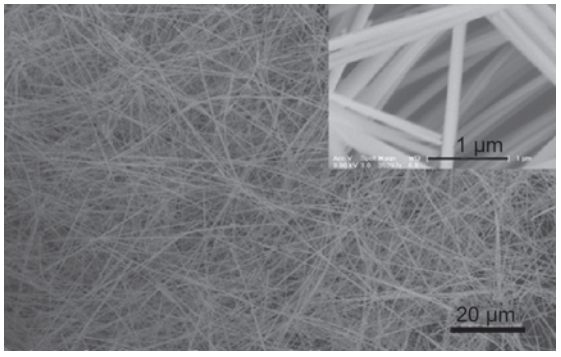

(a)

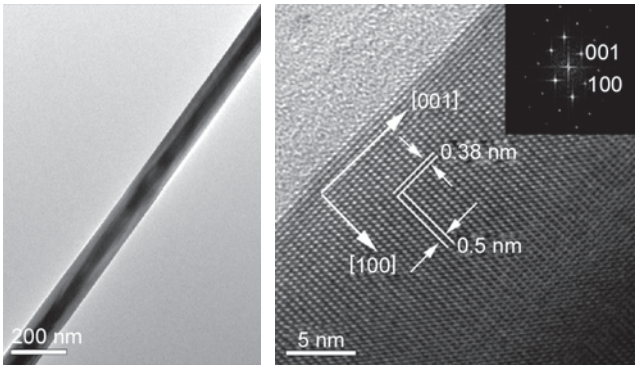

(b) (c)

Figure 7 (a) SEM image of the t-Se nanowires produced by the sonication process. The inset is a high magnification SEM image of the sample; (b) A typical TEM image of the sample; (c) HRTEM image obtained from the edge of the individual Se nanowire sample in (b). The inset in (c) is the fast Fourier transform (FFT) of the HRTEM image

large number of the individual t-Se seeds will result in thinner products. Figure 7(c) displays a high-resolution TEM image of the t-Se nanowires. The fringe spacing (0.5 nm) observed in this image agrees well with the separation of the (001) planes of t-Se, indicating that the as-prepared Se nanowires were structurally single crystals with a growth direction of [001] (*c* axis). The inset of Fig. 7(c) is the fast Fourier transform of the HRTEM image; the symmetrical pattern in the image further confirms the integrity of the single crystal structure. These well-crystallized t-Se nanowires may find potential application in the field of fabricating electronic/optical nanodevices, and also can serve as the templates to generate other functional selenide nanomaterials with one-dimensional shapes.

3. Conclusions

In summary, by utilizing the stability diversity

of Na_2SeSO_3 in different pH environments, we successfully transformed Se powder into monodisperse a-Se spheres through the synthesis and dismutation of Na_2SeSO_3. Subsequently, t-Se nanowires can be prepared by aging these a-Se spheres in ethanol through a "solid-solution-solid" process. The synthesis approach here is simple and straightforward with the precursors being environmentally friendly. This synthetic strategy, which utilizes the stability properties of a precursor, may provide more inspiration in the synthesis of other nanocrystals.

Acknowledgements

This work was supported by NSFC (90606006), the State Key Project of Fundamental Research for Nanoscience and Nanotechnology (2006CB932300) and the Key Grant Project of Chinese Ministry of Education. (NO.306020).

References

[1] Zingaro, R. A.; Cooper W. C. *Selenium*. Van Nostrand-Reinhold: New York, 1974.

[2] Lide, D. V. *Handbook of Chemistry and Physics,* 83rd ed.; CRC Press: Cleveland, 2002.

[3] Berger, L. I. *Semiconductor Materials*; CRC Press: Boca Raton, FL, 1997, p. 86.

[4] Nagels, P.; Sleeckx, E.; Callaerts, R.; Marquez, E.; Gonzalez, J. M.; Bernal-Oliva, A. M. Optical properties of amorphous Se films prepared by PECVD. *Solid State Commun.* **1997**, *102*, 539–541.

[5] Innami, T.; Miyazaki, T.; Adachi, A. Optical constants of amorphous Se. *J. Appl. Phys.* **1999**, *86*, 1382–1387.

[6] Gates, B.; Wu, Y. Y.; Yin, Y. D.; Yang, P. D.; Xia, Y. N. Single-crystalline nanowires of Ag_2Se can be synthesized by templating against nanowires of trigonal Se. *J. Am. Chem. Soc.* **2001**, *123*, 11500–11501.

[7] Jiang, X. C.; Mayers, B.; Herricks, T.; Xia, Y. N. Direct synthesis of Se@CdSe nanocables and CdSe nanotubes by reacting cadmium salts with Se nanowires. *Adv. Mater.* **2003**, *15*, 1740–1743.

[8] Gates, B.; Mayers, B.; Cattle, B.; Xia, Y. N. Synthesis and characterization of uniform nanowires of trigonal selenium. *Adv. Funct. Mater.* **2002**, *12*, 219–227.

[9] Mayers, B. T.; Liu, K.; Sunderland, D.; Xia, Y. N. Sonochemical synthesis of trigonal selenium nanowires. *Chem. Mater*. **2003**, *15*, 3852–3858.

[10] Guatam, U. K.; Nath, M.; Rao, C. N. R. New strategies for the synthesis of t-selenium nanorods and nanowires. *J. Mater. Chem.* **2003**, *13*, 2845–2847.

[11] Guatam, U. K.; Gundiah, G.; Kulkarni, G. U. Scanning tunneling microscopy and spectroscopy of Se and Te nanorods. *Solid State Commun*. **2005**, *136*, 169–172.

[12] Zhang, J.; Zhang, S. Y.; Chen, H. Y. CTAB-controlled synthesis of one-dimensional selenium nanostructures. *Chem. Lett*. **2004**, *33*, 1054–1055.

[13] Liu, X. Y.; Mo, M. S.; Zeng, J. H.; Qian, Y. T. Large-scale synthesis of ultra-long wire-like single-crystal selenium arrays. *J. Cryst. Growth* **2003**, *259*, 144–148.

[14] Smith, T. W.; Cheatham, R. A. Functional polymers in the generation of colloidal dispersions of amorphous selenium. *Macromolecules* **1980**, *13*, 1203–1207.

[15] Zhang, J. S.; Gao, X. V.; Zhang, L. D.; Bao, Y. P. Biological effects of a nano red elemental selenium. *Biofactors* **2001**, *15*, 27–38.

[16] Gao, X. Y.; Gao, T.; Zhang, L. D. Solution-solid growth of α-monoclinic selenium nanowires at room temperature. *J. Mater. Chem.* **2003**, *13*, 6–8.

[17] Mees, D. R.; Pysto, W.; Tarcha, P. J. J. Formation of selenium colloids using ascorbate as the reducing agent. *Colloid Interface Sci*. **1995**, *170*, 254–260.

[18] Lin, Z. H.; Wang, C. R. C. Evidence on the size-dependent absorption spectral evolution of selenium nanoparticles. *Mater. Chem. Phys*. **2005**, *92*, 591–594.

[19] Zhu, Y. J.; Qian, Y. T.; Huang, H.; Zhang, M. W. Preparation of nanometer-size selenium powders of uniform particle size by γ-irradiation. *Mater. Lett*. **1996**, *28*, 119–122.

[20] Jeong, U.; Xia, Y. N. Synthesis and crystallization of monodisperse spherical colloids of amorphous selenium. *Adv. Mater*. **2005**, *17*, 102–106.

[21] Song, J. M.; Zhu, J. H.; Yu, S. H. Crystallization and shape evolution of single crystalline selenium nanorods at liquid-liquid interface: From monodisperse amorphous Se nanospheres toward Se nanorods. *J. Phys. Chem. B* **2006**, *110*, 23790–23795.

[22] Lucovsky, G.; Mooradian, A.; Taylor, W.; Wright, G. B.; Keezer, R. C. Identification of fundamental vibrational modes of trigonal α-monoclinic and amorphous selenium. *Solid State Commun*. **1967**, *5*, 113–117.

[23] Jeong, U.; Xia, Y. N. Photonic crystals with thermally switchable stop bands fabricated from Se@Ag_2Se spherical colloids. *Angew. Chem. Int. Ed*. **2005**, *44*, 3099–3103.

[24] Camargo, P. H. C.; Lee, Y. H.; Jeong, U.; Zou, Z. Q.; Xia, Y. N. Cation exchange: A simple and versatile route to inorganic colloidal spheres with the same size but different compositions and properties. *Langmuir* **2007**, *23*, 2985–2992.

[25] Peng, Q.; Xu, S.; Zhuang, Z. B.; Wang, X.; Li, Y. D. A general chemical conversion method to various semiconductor hollow structures. *Small* **2005**, *1*, 216–221.

[26] Gates, B.; Yin, Y. D.; Xia, Y. N. A solution-phase approach to the synthesis of uniform nanowires of crystalline selenium with lateral dimensions in the range of 10–30 nm. *J. Am. Chem. Soc.* **2000**, *122*, 12582–12583.

[27] Gates, B.; Mayers, B.; Grossman, A.; Xia, Y. N. A sonochemical approach to the synthesis of crystalline selenium nanowires in solutions and on solid supports. *Adv. Mater*. **2002**, *14*, 1749–1752.

[28] Li, Q.; Yam, V. W. W. High-yield synthesis of selenium nanowires in water at room temperature. *Chem. Commun*. **2006**, *9*, 1006–1008.

[29] Xie, Q.; Dai, Z.; Huang, W. W.; Zhang, W.; Ma, D. K.; Hu, X. K.; Qian, Y. T. Large-scale synthesis and growth mechanism of single-crystal Se nanobelts. *Cryst. Growth Des*. **2006**, *6*, 1514–1517.

[30] Li, X. M.; Li, Y.; Li, S. Q.; Zhou, W. W.; Chu, H. B.; Chen, W.; Li, I. L.; Tang, Z. K. Single crystalline trigonal selenium nanotubes and nanowires synthesized by sonochemical process. *Cryst. Growth Des*. **2005**, *5*, 911–916.

[31] Abdelouas, A.; Gong, W. L.; Lutze, W.; Shelnutt, J. A.; Franco R.; Moura, I. Using cytochrome c_3 to make selenium nanowires. *Chem. Mater*. **2000**, *12*, 1510–1512.

[32] Cheng, B.; Samulski, E. T. Rapid, high yield, solution-mediated transformation of polycrystalline selenium powder into single-crystal nanowires. *Chem. Commun.* **2003**, *16*, 2024–2025.

[33] Lu, J.; Xie, Y.; Xu, F.; Zhu, L. Y. Study of the dissolution behavior of selenium and tellurium in different solvents—A novel route to Se, Te tubular bulk single crystals. *J. Mater. Chem.* **2002**, *12*, 2755–2761.

[34] Lee. E. P.; Xia. Y. Growth and patterning of Pt nanowires on silicon substrates. *Nano Res*. **2008**, *1*, 129–137.